PHYSICAL REVIEW B VOLUME 47, NUMBER 9 1 MARCH 1993-I

Analysis of the Ce $3d$-$4d4d$ Auger spectrum with the use of synchrotron radiation

D. D. Sarma*
Institut für Festkörperforschung, Forschungszentrum Jülich, 5170 Jülich, Federal Republic of Germany and Solid State and Structural Chemistry Unit, Indian Institute of Science, Bangalore-560012, India

C. Carbone
Institut für Festkörperforschung, Forschungszentrum Jülich, 5170 Jülich, Federal Republic of Germany

R. Cimino
Istituto Nazionale di Fisica Nucleare, Laboratori Nazionali di Frascati, I-00044 Frascati (Roma), Italy

P. Sen†
Institut für Festkörperforschung, Forschungszentrum Jülich, 5170 Jülich, Federal Republic of Germany

W. Gudat
Berliner Elektronenspeicherring-Gesellschaft für Synchrotronstrahlung, Lentzealle 100, 1000 Berlin 33, Federal Republic of Germany

W. Eberhardt
Institut für Festkörperforschung, Forschungszentrum Jülich, 5170 Jülich, Federal Republic of Germany
(Received 10 August 1992; revised manuscript received 9 November 1992)

We report $3d$-$4d4d$ Auger spectra of Ce metal with the use of synchrotron radiation to excite the initial core hole. By sweeping the excitation energy through the $3d \rightarrow 4f$ threshold, it has been possible to excite different initial states selectively, enabling us to analyze the complex spectrum in terms of different contributions arising from various decay channels.

INTRODUCTION

While the $4d$-VV Auger spectral features from the rare-earth elements have been interpreted[1] in great detail, similar analysis has not been performed for the intense $3d$-$4d4d$ Auger spectral features. The $3d$-$4d4d$ Auger spectra from the rare-earth elements and their compounds are very complex, spanning a wide energy range (more than 100 eV) due to the overlapping intensities from various decay channels and due to the presence of extensive multiplet interactions between the multiply-open levels. Thus a $3d$ core hole ($3d_{5/2}$ or $3d_{3/2}$) can decay by the Auger process $3d^9 4d^{10} 4f^n \rightarrow 3d^{10} 4d^8 4f^n + e$ [see Fig. 1(a)], leading to two sets of Auger signals separated by the spin-orbit splitting of the $3d$ level. However, the various multiplets arising from $4d^8 4f^n$ final states are spread over an energy substantially larger than the spin-orbit splitting of the $3d$ core-hole initial state; this leads to considerable overlap between the $3d_{5/2}$ and $3d_{3/2}$ related Auger features. Further complications arise from the possibility of a Coster-Kronig transition of the $3d_{3/2}$ core-hole state, namely $3d_{3/2} \rightarrow 3d_{5/2} x + e$, where x represents a hole in the $4f$ or $(5d,6s)$ conduction band. Such a transition will be followed by a further Auger decay of the $3d_{5/2}$ core hole thus generated, but in presence of an extra (spectator) hole x in the initial and the final states of the transition. This process is schematically shown in Fig. 1(b). Signals due to these spectator-hole Auger transitions are shifted with respect to the normal ones due to the presence of various Coulomb interactions. The Auger spectra are further complicated if electrons instead of photons are used as a primary source of exciting the initial $3d$ core holes. In this case, the $3d$ electrons instead of being ionized may also be resonantly excited to the $4f$ level, $3d^{10} 4f^n \rightarrow 3d^9 4f^{n+1}$. This $3d$ core-hole state ($3d_{5/2}$ as well as $3d_{3/2}$) will also undergo Auger decay,

$$3d^9 4d^{10} 4f^{n+1} \rightarrow 3d^{10} 4d^8 4f^{n+1} + e \ ,$$

[Fig. 1(c)], contributing different but overlapping Auger signals due to the presence of an extra (or spectator) *electron* in the $4f$ level of the initial and final states. It should be noticed that a Coster-Kronig transition of a

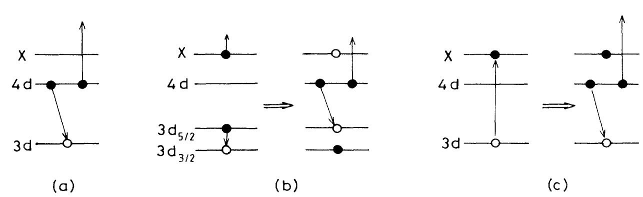

FIG. 1. Schematic representation of the various Auger transitions for a $3d$ core hole in the $3d$-$4d4d$ spectral region. (a) Normal $3d$-$4d4d$ transition; (b) spectator-*hole* Auger transition accompanying $3d_{5/2}$ core hole following a Coster-Kronig $3d_{3/2} - 3d_{5/2} x$ ($x = 4f$ or conduction band) transition; and (c) spectator-*electron* Auger transition following a resonant excitation of a $3d$ electron to the $4f$ level.

 ©1993 The American Physical Society

$3d_{3/2}$ core hole in presence of the resonantly excited $4f$ electron,

$$3d^9(3d_{3/2})4f^{n+1} \rightarrow 3d^9(3d_{5/2})4f^n + e \ ,$$

on the other hand, leads to a $3d_{5/2}$ core hole whose decay produces the normal Auger spectral shape, effectively transferring intensity from the $3d_{3/2}$-related Auger spectra to the $3d_{5/2}$-related Auger spectra. Due to the simultaneous presence of so many different processes contributing intensity in the $3d$-$4d4d$ Auger spectral regions of the rare-earth systems, the resulting spectral features are very complex, making identification of the various processes and the interpretation of the spectral features nearly impossible. However, the tunability of a synchrotron source offers the unique possibility of selectively exciting specific core-hole configurations, thereby identifying Auger signals from various decay processes separately. While there are few studies of Auger transitions in the rare-earth metals using synchrotron radiation,[2,3] we know of no report of systematic study of the evolution of the spectral shapes around the threshold region as a function of photon energy. However such studies have been carried out quite extensively for Auger transitions,[4-8] as well as for the closely related study of x-ray emission spectra[9] from the $3d$ transition metals, using synchrotron radiation. These studies have indeed contributed[4-9] significantly to understanding the origin of the various spectral features in the $3d$ transition-metal case. In the present report we apply this method in order to interpret the $3d$-$4d4d$ Auger spectral features of Ce metal.

EXPERIMENTAL

The experiments were done at the HE-PGM1 beamline of BESSY, Berlin. The monochromator resolution was between 2 and 3 eV depending on the photon energy. The Auger spectra were recorded with a total resolution of 0.5 eV, being independent of the monochromator resolution. The samples were made by evaporating thick films onto a clean iron substrate at room temperature. The base pressure in the chamber was better than 1×10^{-10} mbar and during the evaporation the pressure was better than 5×10^{-10} mbar. The cleanliness of the sample was monitored by recording the photoemission and Auger signals from oxygen and carbon; no trace of these signals could be found in the spectra, indicating very clean samples.

RESULTS AND DISCUSSION

In Fig. 2 we show the Auger spectra of Ce in the $3d$-$4d4d$ region recorded with several photon energies between 878 and 1020 eV. For this purpose, we have normalized all spectra to the same height at the maximum intensities. The spectra show drastic modifications as the photon energy is tuned through the range of 860–900 eV; the spectra with higher photon energies (1010 and 1020 eV) shown in Fig. 2 do not change any further. The spectral changes at lower photon energies are due to the selective opening of different decay channels. In the inset of Fig. 2 we show the $3d$ x-ray-absorption (XA) edge of Ce

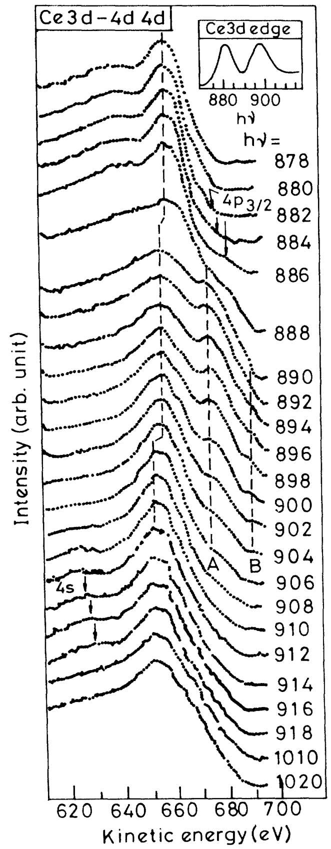

FIG. 2. Ce $3d$-$4d4d$ Auger spectra excited with different photon energies, as indicated. Inset shows the total electron yield spectrum across the $3d$ edge as a function of photon energy.

metal recorded in the total electron yield technique as a reference of the various photon energies used to excite the Auger spectra.

The doublet structure of the $3d \rightarrow 4f$ absorption edge (inset of Fig. 2) corresponds essentially to the excitation of the spin-orbit doublet, $3d_{5/2}$ and $3d_{3/2}$. However, it should be realized here that the states have to be described in terms of the multiplets of the $3d^94f^2$ final state, which is also responsible for the deviation of the intensity ratio of the two peaks in the absorption spectrum from the statistical branching ratio of 3:2. The core-hole decays will be predominantly starting with a $3d^94f^2$ initial state in the vicinity of the resonant excitation energies. Thus the Auger spectras recorded with $h\nu=878$, 880, and 882 eV correspond to an Auger transition $3d^94d^{10}4f^2 \rightarrow 3d^{10}4d^84f^2+e$, which is an Auger transition in presence of a resonantly excited spectator $4f$ *electron* in the initial and final states. The main features in the Auger spectra at this photon energy range are the prominent peak at about 657.5 eV, a broad feature at about 640 eV, and a very weak shoulder at about 673 eV. It should be noted that these features are related to the $3d_{5/2}$ core-hole decay without any contribution from the $3d_{3/2}$ core-hole decay, since the photon energy is insufficient to excite any $3d_{3/2}$ core-hole (see inset of Fig.

2). Moreover, it should be realized that while we identify only the prominent peaks and features in the Auger spectra, presence of extensive multiplet interactions in the multiply-open shells of the Auger process in the rare earths produce signals over the entire spectral range of Fig. 2. Beyond the $3d_{5/2}$ resonant absorption maximum at about 880 eV, the resonant $3d \rightarrow 4f$ excitation probability decreases, leading to a rapid decrease in the intensity of the related Auger spectral features. This decreasing Auger spectral intensity with increasing photon energy beyond 880 eV enables one to observe the otherwise weak 4*p*-related photoemission feature in the Auger spectral range, for example in the spectrum recorded with 886 eV photon energy. These peaks are marked in the figure for some of the photon energies. Unambiguous identification of these features is possible since the kinetic energies for these photoemission signals linearly increase with photon energy.

Beyond 886 eV photon energy, the spectral shape changes very rapidly, as is evident from Fig. 2 where the spectra are shown for every 2-eV increase in the photon energy. First, the spectrum exhibits a marked broadening at 888 eV, the broadening persists in the spectra recorded with 890 and 892 eV photon energies. This broadening is accompanied by a shift of the main peak by nearly 3 eV to about 655 eV kinetic energy (Fig. 2). As the photon energy is increased sufficiently beyond the resonant $3d_{5/2} \rightarrow 4f$ absorption maximum at 880 eV, the resonant absorption process decreases rapidly relative to the normal 3*d* photoionization process. Thus, we should expect the spectator-electron Auger decay to decrease in intensity while the intensity of the normal Auger,

$$3d^9(3d_{5/2})4d^{10}4f^1 \rightarrow 3d^{10}4d^8 4f^1 + e \ ,$$

shows a relative increase with increasing photon energy beyond 880 eV. Thus the broadening of the spectral features at these photon energies is due to the overlap of the two Auger signals of comparable intensities (the normal and the spectator-electron $3d_{5/2}$ Auger). The shift to lower kinetic energies seen in the spectra with 888, 890, and 892 eV photon energies (Fig. 2) are attributed to the emergence of the normal $3d_{5/2}$ core-hole-induced Auger transitions. It should be noted that the normal Auger transition is indeed expected to be at a lower kinetic energy than the spectator-electron Auger signal, however the situation here is considerably complicated by the existence of strong multiplet interactions in the initial and the final states. Moreover, at these photon energies, when the normal $3d_{5/2}$ Auger signal gains intensity, the Auger transition with a spectator electron related to the $3d_{3/2}$ hole also superposes the signal as is discussed below. Beyond 892 eV photon energy, the main peak of the Auger signal remains at 655 eV, though the broadening of the Auger spectrum observed at lower photon energies vanishes. This is due to the vanishing of the $3d_{5/2}$-related spectator-electron Auger intensity compared to the normal Auger signal.

Besides the shift of the maximum and the broadening of the Auger signal, another distinct peak appears at about 674 eV kinetic energy in the Auger spectra excited with 890 eV photon energy (marked *A* in Fig. 2). This peak exhibits a pronounced variation in the intensity as a function of the photon energy across the $3d_{3/2}$ excitation threshold. A similar but weaker intensity feature can also be seen at about 689 eV kinetic energy (marked *B* in Fig. 2). These are evidently Auger signals as these do not shift in energy position with changing photon energy. Moreover the intensities of these two features nearly vanish beyond the resonant absorption energies related to the $3d_{3/2}$ level. Since the resonant absorption process leads to a $4f^2$ configuration as already discussed, these spectral features at 674 and 689 eV kinetic energies are attributed to $3d_{3/2}$-related spectator-*electron* Auger transitions. It should be noted that the more intense $3d_{3/2}$-related spectator-electron Auger signal at 674 eV is at approximately 16.5 eV higher kinetic energy compared to the main peak in the $3d_{5/2}$ related spectator-electron signal at about 657.5 eV (Fig. 2); this energy difference is comparable to the spin-orbit splitting of the Ce 3*d* core level, supporting the above interpretation.

For the spectra recorded with photon energies higher than 904 eV, the distinct spectral features due to the $3d_{3/2}$ spectator-electron Auger nearly vanish (see Fig. 2), with a simultaneous shift in the main Auger peak from 657.5 eV kinetic energy for $h\nu = 886$ to about 651 eV kinetic energy (for $h\nu > 906$ eV) as shown in Fig. 2. This main peak at about 651 eV is attributed to the $3d_{5/2}$-related normal Auger signals. This shift of the normal $3d_{5/2}$ Auger signal compared to the Auger signal with a spectator electron is about 6 eV towards the lower kinetic energy and can easily be understood in terms of the various electron-electron interaction strengths. Since the kinetic energy of the normal Auger transition is given by the total energy difference,

$$E(3d^9 4d^{10}4f^1) - E(3d^{10}4d^8 4f^1) \ ,$$

while that for the Auger transition in presence of a spectator 4*f* electron is given by

$$E(3d^9 4d^{10}4f^2) - E(3d^{10}4d^8 4f^2) \ ,$$

it is easy to see that the average kinetic energy of the Auger electron in the spectator-*electron* process will appear $(2U_{4f} - U_{3f})$ higher than that of the normal Auger; here U_{3f} and U_{4f} are the Coulomb interaction strengths between a 4*f* electron and a 3*d* and 4*d* electron, respectively. Using the values of U_{3f} and U_{4f} estimated earlier,[10,11] we obtain an average energy difference of 5.3 eV between these two signals. Thus the energy shift of the main peak towards lower kinetic energy by approximately 6 eV for the normal Auger transition is in good agreement with the estimates based on the energetics.

At these photon energies, the 4*s* photoemission signal moves through the Auger signal as can be seen in Fig. 2. The Auger spectral features with high photon energies (>900 eV) show the existence of the $3d_{3/2}$-related features only as a continuous extension of the spectra towards higher kinetic energy rather than as a separate peak. However, a weak intensity shoulder can be observed for the spectra recorded with $h\nu = 918$ eV at about 15 eV higher kinetic energy compared to the main $3d_{5/2}$

normal Auger peak. This energy difference being comparable to the spin-orbit splitting of the $3d$ core level in Ce, we attribute this shoulder to the main peak of the normal $3d_{3/2}$ Auger transition. While the spectral features are indeed broad, it does, however, appear that the intensity of the $3d_{3/2}$-related Auger peaks compared to $3d_{5/2}$-related features are weaker than what would be expected on the basis of the degeneracies of the initial core-hole states. This indicates the presence of the Coster-Kronig transitions transferring spectral weight from the $3d_{3/2}$-related features to those associated with the $3d_{5/2}$ initial hole state. At these photon energies, the spectator-hole Auger process

$$3d^9(3d_{3/2})4d^{10}4f^1 \rightarrow 3d^9(3d_{5/2})4d^{10}4f^0+e \rightarrow 3d^{10}4d^8 4f^0+2e$$

should also contribute some intensity, provided that the spectator hole in the $4f$ level has a lifetime comparable to the Auger lifetime of the $3d_{5/2}$ core hole. Once again on the basis of various Coulomb interactions it can be seen that the Auger transition in presence of a spectator $4f$ hole will have $(2U_{4f}-U_{3f})$ lower kinetic energy compared to the normal Auger transition. It should be noticed that a similar process,

$$3d^9(3d_{3/2})4d^{10}4f^2 \rightarrow 3d^9(3d_{5/2})4d^{10}4f^1+e \rightarrow 3d^{10}4d^8 4f^1+2e \ ,$$

around the $3d_{3/2} \rightarrow 4f$ resonance energy will also be present, contributing some further intensity to the normal $3d_{5/2}$-related Auger signal. However, it has been estimated[12] that the contribution to the spectator-hole channel is small in the case of La metal, and we expect it to contribute similarly small intensity to the $3d$-$4d4d$ Auger spectrum of Ce also. The spectator-hole Auger transition will be further weakened by the decay of the spectator hole[7,8] prior to the Auger decay of the $3d$ core hole.

As the photon energy is increased further, the spectral shape becomes slightly broader, as can be seen by comparing the Auger spectrum recorded with 1010 eV photon energy with that recorded with 918 eV (Fig. 2). These extra features are most probably due to a further increase in the photoionization cross section of the $3d_{3/2}$ core hole beyond the threshold energies relative to the $3d_{5/2}$ cross sections.[13] Beyond 1000 eV photon energy we do not observe any further changes in the Auger spectra.

The above assignments, in particular the spectator-electron Auger signals related to the $3d_{3/2}$ core-hole decay, are further supported by the observation of constant-final-state (CFS) spectrum of these Auger

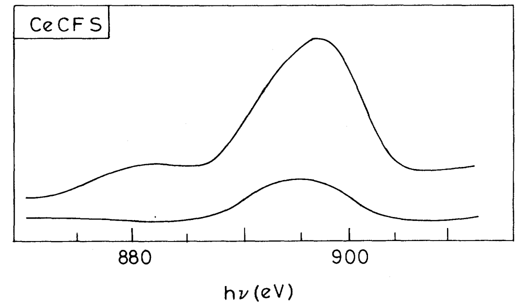

FIG. 3. Constant-final-state spectra or the intensity variation of the two Auger spectral features at 674 eV (peak A in Fig. 2) and at 689 eV (peak B) kinetic energies as a function of photon energy (see text).

features. Thus we have recorded the intensity variation of the spectral features at 674 and 689 eV kinetic energies (peaks A and B in Fig. 2) as a function of photon energy and compared it with that of the background level at about 698 eV kinetic energy. The difference with respect to the background level provides a measure of the true variation of the Auger spectral intensity. These difference CFS spectra at 674 and 689 eV kinetics energies are shown in Fig. 3. These exhibit strong variations in the photon energy range primarily across the $3d_{3/2} \rightarrow 4f$ resonant excitation, indicating that these features are indeed due to the $4f^2$ initial and final states. It should be noted here that even away from the resonant absorption energies, these features are expected to have small but finite intensity. This arises from the fact that the $3d$ core-hole ionization process in Ce metal produces both $3d^9 4f^1$ and $3d^9 4f^2$ final states, the latter with lower probability and arising from core-hole screening.[14]

In conclusion, we have recorded the $3d$-$4d4d$ Auger spectral region in Ce metal with different photon energies across the $3d \rightarrow 4f$ excitation energies. Using the details of the spectral variations with the photon energies along with various energy considerations, it has been possible to analyze the complex spectrum in terms of different contributions arising from the normal Auger decay as well as Auger decay in presence of a spectator electron in the $4f$ level for the $3d_{5/2}$ and $3d_{3/2}$ core-hole states.

ACKNOWLEDGMENTS

We thank the staff of BESSY, in particular Dr. W. Braun, for help during the measurements. One of us (D.D.S.) thanks Forschungszentrum Jülich for hospitality during part of this work.

*Permanent address: Solid State and Structural Chemistry Unit, Indian Institute of Science, Bangalore-560 012, India.
†Permanent address: School of Physical Sciences, Jawaharlal Nehru University, New Delhi-110 067, India.

[1] J. C. Riviere et al., J. Electron Spectrosc. Relat. Phenom. **36**, 331 (1985).
[2] O. P. Sairanen and S. Aksela, J. Phys. Condens. Matter **4**, 3337 (1992).
[3] J. A. D. Matthew, R. Dudde, and F. P. Netzer, J. Electron Spectrosc. Relat. Phenom **56**, 365 (1991).
[4] D. D. Sarma, C. Carbone, P. Sen, R. Cimino, and W. Gudat, Phys. Rev. Lett. **63**, 656 (1989); **66**, 967 (1991).

[5]D. D. Sarma, C. Carbone, P. Sen, and W. Gudat, Phys. Rev. B **40**, 12 542 (1989).

[6]S. B. Whitefield, G. Bradley Armen, R. Carr, J. C. Levin, and B. Crasemann, Phys. Rev. B **37**, 419 (1988).

[7]D. D. Sarma, R. Cimino, C. Carbone, P. Sen, S. R. Barman, and W. Gudat, Phys. Scr. **T41**, 187 (1992).

[8]D. D. Sarma, S. R. Barman, R. Cimino, C. Carbone, P. Sen, A. Roy, A. Chainani, and W. Gudat (unpublished).

[9]N. Wassdahl, J. E. Rubensson, G. Bray, P. Glans, P. Bleckert, R. Nyholm, S. Cramm, N. Martensson, and J. Nordgren, Phys. Rev. Lett. **64**, 2807 (1990).

[10]J. F. Herbst and J. W. Wilkins, Phys. Rev. Lett. **43**, 1760 (1979).

[11]D. D. Sarma and P. V. Kamath, Phys. Rev. B **36**, 7402 (1987).

[12]S. J. Oh, G. H. Kim, G. A. Sawatzky, and H. T. Jonkman, Phys. Rev. B **37**, 6145 (1988).

[13]J. J. Yeh and I. Lindau, At. Data Nucl. Data Tables **32**, 1 (1985).

[14]J. C. Fuggle, M. Campagna, Z. Zolnierek, R. Lasser, and A. Platau, Phys. Rev. Lett. **45**, 1597 (1980).